Applied Catalysis B: Environmental 219 (2017) 142–154

Contents lists available at ScienceDirect

Applied Catalysis B: Environmental

journal homepage: www.elsevier.com/locate/apcatb

Effect of gas compositions on SO_2 poisoning over Cu/SSZ-13 used for NH_3-SCR

Kurnia Wijayanti[a], Kunpeng Xie[a], Ashok Kumar[b], Krishna Kamasamudram[b], Louise Olsson[a,*]

[a] Competence Centre for Catalysis, Chemical Engineering, Chalmers University of Technology, SE-41296 Gothenburg, Sweden
[b] Cummins Inc., 1900 McKinley Ave, MC 50183, Columbus, IN 47201, USA

ARTICLE INFO

Article history:
Received 19 January 2017
Received in revised form 30 June 2017
Accepted 8 July 2017
Available online 10 July 2017

Keywords:
Sulfur poisoning
Cu/SSZ-13
Cu zeolites
TPD
XPS
UV–vis

ABSTRACT

This study focuses on the effect of gas composition during SO_2 poisoning over Cu/SSZ-13 for NH_3-SCR application and was performed by conducting SO_2-TPD experiments in a variety of lean gas compositions. In addition, the poisoned monoliths were characterized in detail using ICP-SFMS, UV–vis and XPS. During SO_2 poisoning under dry and lean conditions, two different sulfur species were found, which were assigned to weakly bound SO_2 and copper sulfate like species. Moreover, a significantly larger amount of copper sulfates was present in humid environment. The presence of NH_3 during the poisoning resulted in the formation of ammonium sulfate species which were decomposed at the same temperature independently if the poisoning with SO_2 was conducted in ammonia oxidation conditions or under standard or fast SCR conditions. Moreover, if the temperature ramp was conducted with O_2 and H_2O compared to Ar alone, more stable sulfate species were formed. In addition, SO_2 poisoning under standard SCR conditions resulted in mostly ammonium sulfate formation at 200 °C, whereas copper sulfates were predominant after poisoning at 400 °C. After hydrothermal aging at 800 °C, more reducible copper species were noticeable and UV–vis showed that copper oxides had been formed. Sulfur poisoning of the hydrothermally aged sample resulted in the additional formation of copper sulfates during poisoning at 200 °C, which was not the case for poisoning of the fresh catalyst. Thus, the copper oxide species enhanced the copper sulfate formation.

1. Introduction

Ammonia selective catalytic reduction (SCR), in which aqueous urea is used as a reductant, is a commonly practiced technology to reduce NO_x in diesel vehicles. For this application, the popularity of vanadia supported on a titania catalyst has been substituted by metal-exchanged zeolites because of its sensitivity towards hydrothermal aging [1]. Among metal-exchanged zeolites, Fe-zeolites are more active in the high temperature region whereas copper zeolites offer high activity at lower temperature [2]. In the last few years, focus of the research has turned to copper chabazite catalysts (Cu/CHA) [3], such as Cu/SSZ-13 and Cu/SAPO-34 because of their resistance towards hydrothermal aging [4–6] and hydrocarbon poisoning [7,8]. The activities of the Cu/CHA catalysts rely on the copper sites which are suggested to occupy two different cationic positions [9]. Distribution of the copper sites in these positions, i.e. inside the six-membered ring (6R) and in the large zeolite cages (in the 8MR), is determined primarily by the copper loading [9,10]. Understanding the nature and behavior of the active copper sites can be useful to design improved NH_3-SCR system that has minimal effect of sulfur poisoning.

Studying the impact of sulfur poisoning on the catalyst system is crucial because of the unavoidable presence of sulfur in the fuel. The copper-based catalyst has shown to be more prone to poisoning by sulfur compared to Fe-zeolite [11–13]. Several studies [12–17] have been published regarding this subject and several factors are proven to be important in the deactivation of the copper zeolites caused by SO_2. Decreasing activity of the catalysts is mainly observed at low temperatures [12–16] where the Cu-zeolite SCR catalysts have performance advantage over other SCR catalysts [12]. The degree of impact of SO_2 poisoning on the different reactions is not the same, e.g. the standard SCR reaction is more affected by the poisoning than the fast SCR reaction [11,14,15]. When the ratio of NO_2/NO_x in the SCR is higher than 0.5, the impact is even less than in the fast SCR case [14,15].

* Corresponding author.
E-mail address: louise.olsson@chalmers.se (L. Olsson).

http://dx.doi.org/10.1016/j.apcatb.2017.07.017
0926-3373/

Results from several research studies [14,15,18–24] have highlighted important mechanistic information regarding sulfur poisoning of copper zeolite catalysts in the NH_3-SCR system. Since SO_2 is expected to have higher affinity to the copper species than to the strong acid sites of the zeolite [18], the deactivation caused by SO_2 is believed to be correlated with the sulfur species bound to copper sites. This fact is in accordance with our previous finding [15] which indicates that the reducibility of copper in Cu/SAPO-34 decreased during an H_2-TPR experiment after it had been exposed to SO_2 in the presence of O_2 and H_2O. In addition, Cheng et al. [19] observed that sulfate species were formed after the Cu/BEA sample had been poisoned with SO_2. Moreover, Hamada et al. [20] found similar result using Cu/ZSM-5 catalyst and they suggested that the electronic and local structure of the Cu species of sulfur poisoned sample changed, possibly caused by the presence of sulfate ions in the surroundings of Cu ions, which then blocked the NO adsorption. This claim is also supported by Hass and Schneider [21], who performed DFT calculations showing that complexes, such as ZCu-SO_4 or ZCu–SO_4–CuZ, were formed during SO_2 exposure under O_2 excess conditions and these complexes were significantly different compared to bulk $CuSO_4$.

It has been observed that the presence of other gases during SO_2 poisoning influences the type of sulfur species formed; for example, during sulfur poisoning in the presence of NH_3, as investigated by Zhang et al. [22], ammonium sulfate species were observed over Cu/SAPO-34 and the formed ammonium sulfate species then poisoned the active sites and blocked the zeolite pores. The pore blocking mechanism has also been observed in our previous studies [14,15] denoted by a decreasing surface area of the sulfur poisoned catalysts. In a recent study, Wang et al. [23] characterized different species present during SO_2 poisoning over Cu/SAPO-34 in NO oxidation and SCR conditions at various temperatures. Based on their experiments, it was found that copper sulfate was present in all sulfated samples, whereas ammonia sulfate was only found after the samples poisoned with SO_2 in SCR environment at 250 °C (but not at 350 °C). Moreover, it has been found that the activity of the catalyst can be regained by heating up the poisoned sample [19,25,26] even though a temperature of 500 °C is insufficient to fully recover the catalytic activity [15]. The recoverability also depends on the form of sulfur in the feed; the presence of SO_3 at high temperature results in greater difficulties in regenerating the catalyst and SO_3 also causes a more severe effect on the catalytic activity than SO_2 [26]. Moreover, Kumar et al. [27] found that SCR conditions might enhance sulfur regeneration.

There are several studies examining the sulfur poisoning over Cu/SAPO-34 [15,17,18,22–24], however there are only few studies focusing on sulfur poisoning of Cu/SSZ-13 [14,16,28,29]. Both Cu/SAPO-34 and Cu/SSZ-13 have CHA structure, but there are several differences between these two materials. For example, Cu/SAPO-34 produces less N_2O and forms more stable ammonium nitrates compared to Cu/SSZ-13 [31]. In a recent study by Su et al. [28], they found during sulfur TPD experiments, that the sulfur release (from 200 to 1000 °C) was about double for Cu/SSZ-13 compared to Cu/SAPO-34, which demonstrates that poisoning of Cu/SSZ-13 is different from Cu/SAPO-34 and it is therefore critical to also study sulfur poisoning of Cu/SSZ-13 in detail.

In our previous investigation [14], we showed that SO_2 poisoning under SCR conditions over Cu/SSZ-13 results in more severe poisoning than sulfur treatment with O_2 and H_2O alone; however, the question of what specifically occurs during SO_2 deactivation in different gas compositions requires further study. To our knowledge, there are no studies available that have used different surface characterization techniques to examine the sulfur species when poisoning the Cu/SSZ-13 catalyst using various gas compositions, which is the objective of the current study. In this work, we characterized the formed sulfur species over Cu/SSZ-13 during different conditions using UV–vis and XPS and examined the stability using the TPD technique. Dry and humid conditions are used, as well as under ammonia oxidation, standard SCR and fast SCR conditions. In addition, the effect of sulfur poisoning in combination with hydrothermal aging was also investigated in this study.

2. Experimental

2.1. Catalyst synthesis

The Cu/SSZ-13 catalyst used in this study was prepared by an ion exchange of Na/SSZ-13 which was synthetized based on the procedure adopted from McEwen et al. [29], which has been described in detail in our earlier studies [30,31]. First, the Na/SSZ-13 underwent two steps of ammonium exchange by stirring 30-g zeolite into a solution of 1000 mL of 2 M NH_4NO_3 (99% Sigma Aldrich) at 80 °C for 15 h. The zeolite was then filtered, washed several times with deionized water and the resulting powder was dried at 80 °C for 12 h. Following this procedure, copper exchange was performed in 0.2 M $Cu(NO_3)_2$ (98%, Alfa Aesar GmbH) at 80 °C at a 100:3 ratio of solution to zeolite. After 1 h of stirring, the zeolite was separated from the solution and washed with deionized water until it became neutral. Thereafter, the copper exchange was repeated three times and the resulting Cu/SSZ-13 was dried at 80 °C for 12 h and calcined at 550 °C for 4 h (ramp speed of 5 °C min^{-1}). Surface area and pore volume of the in-house synthesized Cu/SSZ-13 were measured using the N_2 physisorption method (Micromeritics ASAP 2010) resulting in 504 $m^2\ g^{-1}$ and 0.25 $cm^3\ g^{-1}$, respectively. In addition, an elemental analysis using the inductively coupled plasma sector field mass spectrometer (ICP-SFMS) was performed by ALS Scandinavia AB, with the result showing that fresh Cu/SSZ-13 powder contained 7.3 wt.% Cu, Si/Al ratio of 3.64 and Cu/Al of 0.39 (resulting in an ion exchange of 78%).

The Cu/SSZ-13 powder was then washcoated onto cordierite monoliths possessing a cell density of 400 cpsi, 14 mm in diameter and 20 mm in length. The monoliths were dipped into a solution consisting of 20 wt.% solid phase (ratio of catalyst to boehmite (Disperal P2, Sasol, GmbH) of 95:5) and 80 wt.% liquid phase (ratio water to ethanol of 1:1), followed by an air drying at 90 °C for 2 min and a short time calcination at 500 °C for 2 min. This step was repeated several times and thereafter, the monoliths were calcined in an oven at 500 °C for 2 h (ramp speed of 5 °C min^{-1}). The final weight of the washcoat in each monolith was approximately 250 mg (including the binder). These prepared monoliths were then used for TPD experiments in the flow reactor and for characterization purposes (ICP-SFMS, XPS and UV-vis).

2.2. Temperature-programmed desorption (TPD) experiment

The TPD experiments were performed in a flow reactor set-up as described elsewhere [14]. Briefly, it consisted of a gas dosing system (Bronkhorst mass flow controllers), a system for controlling water vapor flow and a horizontal quartz tube (1.6 cm in diameter and 70 cm in length) into which the catalyst was inserted. Two type-K thermocouples were used to measure the temperature in the gas flow before the catalyst and in the center of the middle channel. A gas Fourier transform infrared (FTIR) spectrometer (MKS Multigas 2030) with a pair of zinc selenide (ZnSe) windows was connected to the outlet of the reactor for monitoring the gas concentration. The lines prior to and after the reactor had been heated to 200 °C were well insulated in order to prevent sulfur condensation during measurements. All experiments performed in the flow reactor used a total flow of 1200 mL min^{-1}, corresponding to 17,900 h^{-1} gas hourly space velocity (GHSV) and Argon was used as inert balance.

Table 1
TPD experiment performed with Cu/SSZ-13 catalyst. In all experiments where O_2 and H_2O are present the concentrations were 8 and 5%, respectively.

TPD	Adsorption		Isothermal desorption	Desorption
	Gas composition	T (°C)		Ramp to 900 °C
1	$SO_2 + O_2$	200	Ar	Ar
2	$SO_2 + O_2 + H_2O$	200	Ar	Ar
3[a]	$SO_2 + O_2 + H_2O + NH_3$	200	Ar	Ar
4[b]	$SO_2 + O_2 + H_2O + NH_3 + NO$	200	Ar	Ar
5[c]	$SO_2 + O_2 + H_2O + NH_3 + NO + NO_2$	200	Ar	Ar
6[b]	$SO_2 + O_2 + H_2O + NH_3 + NO$	200	$Ar + O_2 + H_2O$	$Ar + O_2 + H_2O$
7[b]	$SO_2 + O_2 + H_2O + NH_3 + NO$	400	$Ar + O_2 + H_2O$	$Ar + O_2 + H_2O$
8[b]	$SO_2 + O_2 + H_2O + NH_3 + NO$ (aged)	200	Ar	Ar

[a] Gas concentration used: 30 ppm SO_2, 8% O_2, 5% H_2O, 400 ppm NH_3 (ammonia oxidation condition).
[b] Gas concentration used: 30 ppm SO_2, 8% O_2, 5% H_2O, 400 ppm NH_3 + 400 ppm NO (standard SCR condition).
[c] Gas concentration used: 30 ppm SO_2, 8% O_2, 5% H_2O, 400 ppm NH_3, 200 ppm NO, 200 ppm NO_2 (fast SCR condition).

In this study, we applied several TPD procedures (marked as TPD 1, TPD 2, etc.), as listed in Table 1, and a fresh catalyst was used for each TPD experiment. In order to obtain stable activity, the catalyst was first degreened using 400 ppm NH_3, 400 ppm NO, 8% O_2 and 5% H_2O at 600 °C for 1 h followed by 20 min of exposing the catalyst to 8% O_2 and 5% H_2O at 600 °C to clean its surface. The TPD procedure consisted of an adsorption of 30 ppm SO_2 and 8% O_2 in the presence of various gases (see Table 1 for details) with an Argon balance at 200 or 400 °C for 3 h. Thereafter, at the same temperature as the adsorption step, the catalyst was flushed with Ar (or 8% O_2, 5% H_2O in Ar) for 30 min to remove loosely bound and adsorbed species from the surface. The temperature was then linearly increased to 900 °C at a ramp speed of 20 °C min^{-1} and finally, the temperature was kept at 900 °C for 10 min. It is not expected during normal diesel operation to reach 900 °C, but this high temperature was chosen in order to desorb all species and get a fundamental understanding of the stability of the sulfur species.

It is worth noting that prior to the adsorption–desorption experiment for the TPD 8, the catalyst was aged at 800 °C for 4 h with 400 ppm NH_3, 400 ppm NO, 8% O_2 and 5% H_2O and, thereafter, the temperature was decreased to 600 °C at which temperature the catalyst was exposed to 8% O_2 and 5% H_2O for 20 min to clean the surface.

2.3. Characterization

For characterization purposes, the adsorption experiments were conducted in the flow reactor, described in Section 2.2, using separate monoliths. First, the catalyst underwent degreening using 400 ppm NH_3, 400 ppm NO, 8% O_2 and 5% H_2O at 600 °C for 1 h followed by exposing it to 8% O_2 and 5% H_2O for 20 min to clean the surface. Thereafter, the adsorption step of the TPD procedure (TPD 1, TPD 2, etc.), as listed in Table 1, was performed. As the adsorption step for TPD 4 and TPD 6 are exactly the same, for characterization purposes the procedure for the latter was not conducted. Following this, the catalyst was then exposed to Ar for 30 min and, finally, the temperature was decreased. In addition, using another monolith, a hydrothermal aging experiment was performed at 800 °C for 4 h using the same procedure and this monolith did not undergo the sulfur adsorption experiment after the aging. It should be noted that a fresh sample was used for each experiment. These monoliths were then cut into two parts along the axial direction. One part of the monolith was used for ICP-SFMS analysis, whereas the other half was used for UV–vis and XPS measurements. The part of the monolith used for the ICP-SFMS measurement was then cut into two pieces perpendicularly to the flow direction of the gas in the reactor and denoted as inlet and outlet. The inlet and outlet referred to the positions of the monolith in the flow reactor according to the gas flow. These samples were then crushed and the sulfur content was measured with ICP-SFMS.

The nature of the different copper species was examined by UV–vis spectroscopy using a Varian Cary 500 instrument with an integrating sphere (Internal DRA 2500). Parts of the poisoned monoliths were physically ground in a mortar and the reflectance were measured with a data interval of 1 nm and a scan rate of 600 nm min^{-1}. Besides the samples, some reference materials, Cu(II) hydroxide (technical grade, Sigma Aldrich), Cu(II) oxide (98%, Sigma Aldrich), Cu (II) sulfate pentahydrate (p.a., Sigma Aldrich) were also measured. The spectra of the reference materials are useful for comparison purposes during data interpretation.

The X-ray photoelectron spectroscopy (XPS) measurement was performed using a PerkinElmer PHI 5000C ESCA system to assess the presence of sulfur species on the samples which underwent adsorption experiment. A small piece of sample trimmed from the inlet half of the monolith was placed on a carbon pad situated on a sample holder and loaded on the load-lock. After the ion gauge had dropped to 2×10^{-8} torr, the sample holder was moved into the ultrahigh vacuum chamber. When the chamber pressure had decreased to 3×10^{-9} torr, the XPS spectra were collected using a monochromatic K α source. The charge correction was performed by shifting the binding energy (BE) using the C 1s peak at 284.6 eV as the reference.

In order to identify the different redox behavior of the copper ions due to hydrothermal aging, a hydrogen temperature-programmed reduction (H_2-TPR) was performed using 100 mg crushed monolith samples of the fresh and aged catalysts. The experiments were conducted in a calorimeter set-up as described earlier in [14,15]. Several Bronkhorst mass flow controllers (MFCs) were used to dose the inlet gases, whereas the outlet gas was monitored by a Hiden HPR-20 QUI mass spectrometer (MS). The total flow was 20 mL min^{-1} and Ar was used as inert balance. Prior to the experiment, the sample was pretreated with 8% O_2 at 600 °C for 20 min to clean the surface and remove the moisture. Thereafter, 3000 ppm H_2 was introduced at 50 °C for 50 min followed by a temperature ramp of 10 °C min^{-1} up to 800 °C while keeping the exposure to H_2. The temperature was then maintained at 800 °C for 40 min with H_2 flow.

3. Result and discussion

3.1. Effect of water presence

As one of the products during fuel combustion, water is always present in the exhaust aftertreatment system. In order to understand the effect of water, we performed TPD experiments where the sulfur poisoning was performed in dry and humid environments (TPD 1 and TPD 2; see Table 1), respectively, and the results are presented in Fig. 1. For TPD 1, the adsorption step was performed by exposing the Cu/SSZ-13 sample to 30 ppm SO_2 and 8% O_2 at 200 °C for 3 h and as shown in Fig. 1A, only a small amount

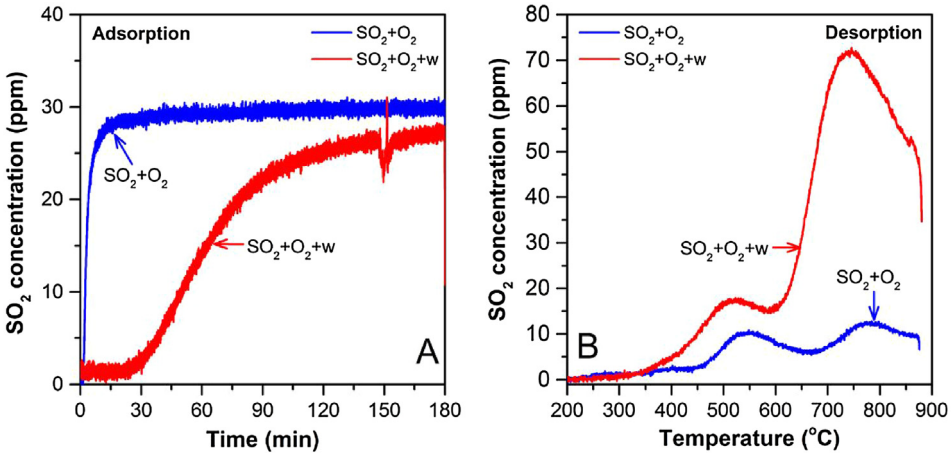

Fig. 1. Outlet concentration of SO_2 during (A) adsorption of 30 ppm SO_2, 8% O_2 (TPD 1) and 30 ppm SO_2, 8% O_2, 5% H_2O (w) (TPD 2) at 200 °C for 3 h followed by flushing the catalyst with Ar only for 30 min. SO_2 concentration during temperature ramp (20 °C min^{-1}) is shown in (B).

of SO_2 was adsorbed on the catalyst as denoted by the SO_2 breakthrough occurring after approximately one min. After the storage period, the catalyst was flushed with Ar for 30 min, followed by a linear increase of the temperature up to 900 °C, where the SO_2 desorption is displayed in Fig. 1B. Two peaks of maxima at around 540 and 780 °C were identified which might be attributable to the presence of weakly bound sulfur and copper sulfate species, respectively. Our results are in line with the study by Zhang et al. [22], where experiments using a commercial Cu/SAPO-34 catalyst also resulted in two distinct peaks following SO_2 adsorption under lean conditions which they attributed to SO_2 chemisorbed on the catalyst surface for the low temperature peak and decomposition of metal sulfate species for the high temperature SO_2 peak. Moreover, referring to a study by Shen et al. [18] showing that almost no sulfur was found on the SAPO-34 after sulfur treatment, it is unlikely that sulfur is attached to the Brönsted acid sites of the zeolite. It is, therefore, probable that both chemisorbed SO_2 as well as sulfate species resides on the copper sites. This is also supported by our previous investigation [15] showing that the reducibility of the copper in the Cu/SAPO-34 during H_2-TPR decreased after sulfur poisoning, which indicates a loss of copper sites due to sulfur poisoning. It is worth noting that the mol balance analysis between SO_2 stored and released shows 102%, thus in excellent agreement (0.042 and 0.043 mol SO_2/mol Cu were adsorbed and desorbed, respectively). According to the ICP-SFMS measurement, no sulfur was left on the sample after it had undergone the TPD experiment, which is expected from the sulfur balance.

In another experiment (TPD 2, see Table 1), water was added to the inlet gas during the sulfur storage period. A different profile, as seen in Fig. 1A, is observed when poisoning is conducted under humid conditions, where a total uptake of SO_2 occurred for about 20 min before the breakthrough was seen. This means that in a lean environment, substantially more sulfur is stored under humid conditions than in a dry environment. As expected, when the temperature was increased, two major peaks were observed and those peaks were significantly higher compared to the TPD 1. This result is consistent with the adsorption period by which an increase in sulfur storage was noted for the experiment under humid conditions. An investigation by Huang et al. [32] using vanadium oxide has shown that the deactivation rate due to sulfur poisoning increased with increasing H_2O content in the inlet gas. Further, this study also demonstrated that the rate of sulfate formation, which is the main reason for sulfur deactivation, was faster when the concentration of H_2O was higher. Despite the fact that the catalyst that Huang et al. [32] used was different from the present study, we suggest that a similar reason could be applicable also to Cu zeolites. Indeed, the TPD showed that the high temperature peak, which we suggest to be due to copper sulfates, is increasing the most in the presence of water. Based on the calculation of the mol balance, 0.423 mol SO_2/mol Cu was adsorbed and only 0.201 mol SO_2/mol Cu was released during the temperature ramp. The ICP analysis of the catalyst after the TPD showed no residual sulfur; thus, it is likely that some of the sulfate species reacted with the water and was further converted into H_2SO_4, which is difficult to be detected in our system. Nevertheless, our results clearly show a dramatical increase of sulfur storage in the presence of water. Moreover, these results clearly show the importance of studying sulfur poisoning of copper zeolites in the presence of water.

In addition, ICP-SFMS measurements were conducted after poisoning only on characterization monoliths and the results are listed in Table 2. These data show the same trend, where much more sulfur was deposited on the sample that underwent the SO_2 storage under humid conditions compared to the experiment in the absence of water. The sulfur deposited on the inlet part of the TPD 2 sample was 1.5 wt.%, compared to 0.6 wt.% for TPD 1. The same trend was observed for the outlet part of the monoliths. Moreover, the sulfur concentration was slightly lower in the outlet part of the monolith, implying that the catalyst is saturated by sulfur from the inlet part moving towards the outlet of the monolith, which is in agreement with our previous observation [14]. However, the differences between the inlet and outlet are quite small for these gas compositions; thus, the monoliths are close to being saturated.

In order to examine the different copper species in the samples, ex-situ UV–vis measurements were performed and the spectra are presented in Fig. 2A in which the sulfur adsorbed samples are compared with the fresh catalyst. In brief, the spectras of the Cu/SSZ-13 samples show two distinct bands: a broad band centered at around 830 nm and another absorption band with maxima at 220 nm. The former is assigned to the d–d transition of Cu^{2+} ions [33–35] in octahedral coordination [35], whereas the other band at 220 nm is ascribed to the ligand charge metal transfer (LMCT) O → Cu caused by the isolated Cu^{2+} [33–35]. In our previous study for Cu/BEA, we observed that the spectra for the catalyst agreed very well with $Cu(OH)_2$ and based on this finding, we proposed that the copper in air mainly exists in the form of hydroxyls [36]. The results in Fig. 2 also show that our fresh Cu/SSZ-13 resembles a similar trend as the reference material $Cu(OH)_2$ (Fig. 2B); thus, the copper in Cu/SSZ-13 is also likely in the form of copper hydroxyls. After the SO_2 storage in dry and lean environment had been conducted, a higher intensity was observed for the absorption band at low wave

Table 2
Sulfur content measured by ICP-SFMS. In all experiments where O_2 and H_2O are present the concentrations were 8 and 5%, respectively.

TPD	Adsorption step		Sulfur content (wt.%)	
	Inlet gas	T (°C)	Inlet	Outlet
1	$SO_2 + O_2$	200	0.6	0.4
2	$SO_2 + O_2 + H_2O$	200	1.5	1.4
3[a]	$SO_2 + O_2 + H_2O + NH_3$	200	2.2	1.4
4[b]	$SO_2 + O_2 + H_2O + NH_3 + NO$	200	2.3	1.4
5[c]	$SO_2 + O_2 + H_2O + NH_3 + NO + NO_2$	200	2.0	2.0
7[b]	$SO_2 + O_2 + H_2O + NH_3 + NO$	400	1.6	1.3
8[b]	$SO_2 + O_2 + H_2O + NH_3 + NO$ (aged 800)	200	1.4	2.3

[a] Gas concentration used: 30 ppm SO_2, 8% O_2, 5% H_2O, 400 ppm NH_3 (ammonia oxidation condition).
[b] Gas concentration used: 30 ppm SO_2, 8% O_2, 5% H_2O, 400 ppm NH_3 + 400 ppm NO (standard SCR condition).
[c] Gas concentration used: 30 ppm SO_2, 8% O_2, 5% H_2O, 400 ppm NH_3, 200 ppm NO, 200 ppm NO_2 (fast SCR condition).

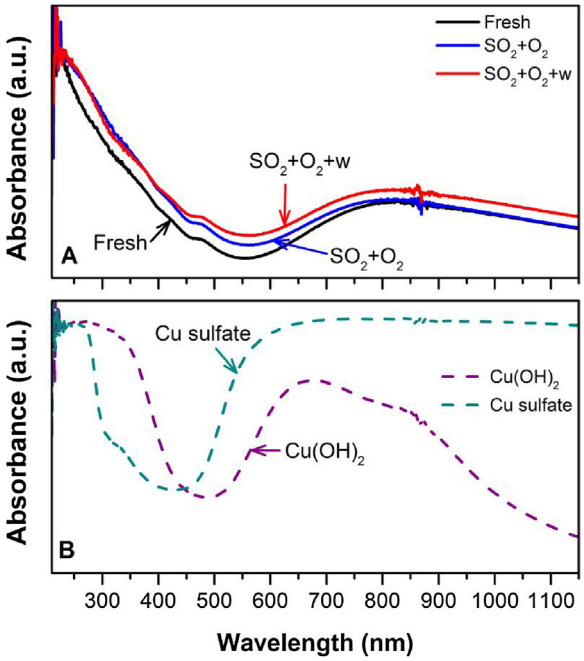

Fig. 2. UV–vis spectra of fresh catalyst and samples that underwent SO_2 storage with ($SO_2 + O_2$) and ($SO_2 + O_2 + H_2O$ (w)) at 200 °C for 3 h (A) in comparison with $Cu(OH)_2$ and Cu sulfate as the reference material (B). The gas concentration during storage experiment was 30 ppm SO_2, 8% O_2, and 0 or 5% H_2O.

lengths implying that Cu^{2+} was affected by the sulfur poisoning under dry conditions, whereas only a minor impact was observed for spectra around 1150–700 nm. Interestingly, when the SO_2 storage was performed under humid conditions, higher absorbance intensities were observed across the entire range of measurement (1150–200 nm); thus, the poisoning altered both absorption bands. Our results, therefore, show a more pronounced poisoning effect on the copper species under humid conditions than in the dry environment. This fact indicates that additional sulfur species were found in the former, which was in line with the result from both the TPD experiments and ICP-SFMS analysis. Moreover, considering that the spectra of Cu sulfate at 1150–500 nm had a higher absorbance intensity compared to that of $Cu(OH)_2$ (Fig. 2B) and that a similar trend was observed for the sulfur poisoned sample under humid conditions, it indicates that copper sulfate species existed on that sample, which was supported by the TPD experiment (Fig. 1). It is worth noting that the copper sulfate formed is likely not derived from the bulk phase as there are clear differences between the UV–vis spectra for the sample and the bulk material. This is in accordance with the DFT simulations performed by Hass and Schneider [21], in which they showed that complexes such as ZCu–SO_4 or ZCu–SO_4–CuZ were formed during SO_2 and O_2 exposure and that these complexes are significantly different from bulk $CuSO_4$.

Further characterization of the sulfur species was conducted using XPS and the spectra of the samples that underwent different sulfur storage experiments compared with the fresh sample are presented in Fig. 3. The primary XPS region for sulfur is 2p, a region close to the position of Si 2s, and the broad background peak observed in the fresh sample (Fig. 3A) is attributable to the surface plasmon emission from Si 2s caused by emission of Si 2s [37], not due to the presence of sulfur because there was no sulfur loaded on this sample. Further, when comparing spectra for fresh and sulfur poisoned samples, the narrower band for sulfur 2p can be easily seen. As shown in Fig. 3, the spectra of the samples poisoned by SO_2 and O_2 both under dry and humid conditions had one single peak with maxima around 169.7 eV, indicating the presence of sulfate species (171.2–168.4 eV [38]) and no other species, including sulfite (165.5–167.5 eV [38]) or sulfide (160.5–164 eV [38]) were detected. A previous investigation by Cheng et al. [19] also found a similar result where only sulfate compounds were observed after the catalyst had been loaded with sulfur.

3.2. Effect of NH_3 presence

The effect of NH_3 during SO_2 poisoning under lean conditions over Cu/SSZ-13 was investigated by performing an adsorption–desorption experiment in which 30 ppm SO_2, 8% O_2, 5% H_2O and 400 ppm NH_3 were fed into the reactor at 200 °C for 3 h during the storage period (TPD 3, see Table 1). The SO_2 concentration during the adsorption period of three experiments are presented in Fig. 4A, where the samples were poisoned in (i) $SO_2 + O_2$ (TPD 1; see Table 1), (ii) $SO_2 + O_2 + H_2O$ (TPD 2) and (iii) $SO_2 + O_2 + H_2O + NH_3$ (TPD 3). The total uptake of SO_2 was about 45 min during SO_2 adsorption with NH_3 present in the inlet gas which is considerably longer than the experiments without NH_3 (1 and 20 min for TPD 1 and TPD 2, respectively). This outcome is in accordance with the result from the ICP-SFMS measurements, which are presented in Table 2, where significantly more sulfur was observed when the inlet gas contained NH_3 (2.2 wt.% S in inlet part of TPD 3 compared to 1.5 and 0.6 wt.% S for TPD 2 and TPD 1, respectively). Interestingly, there was a substantial difference between the inlet and outlet part of the monolith for TPD 3, where the outlet only contained 1.4% sulfur. These results indicate that the monolith had not been saturated with sulfur during this experiment, something that is also seen in Fig. 4A, where the SO_2 concentration has not reached the inlet concentration at the end of the storage phase.

As expected, when the temperature was ramped up, a huge SO_2 peak appeared, which occurred at 420 °C with the onset temperature at about 305 °C. Thus, the main desorption peak is significantly lower than both TPD 1 and TPD 2 (Fig 4B) but in addition, some sulfur was also released at higher temperature. We suggest that the SO_2 peak observed is caused by the decomposition of the ammo-

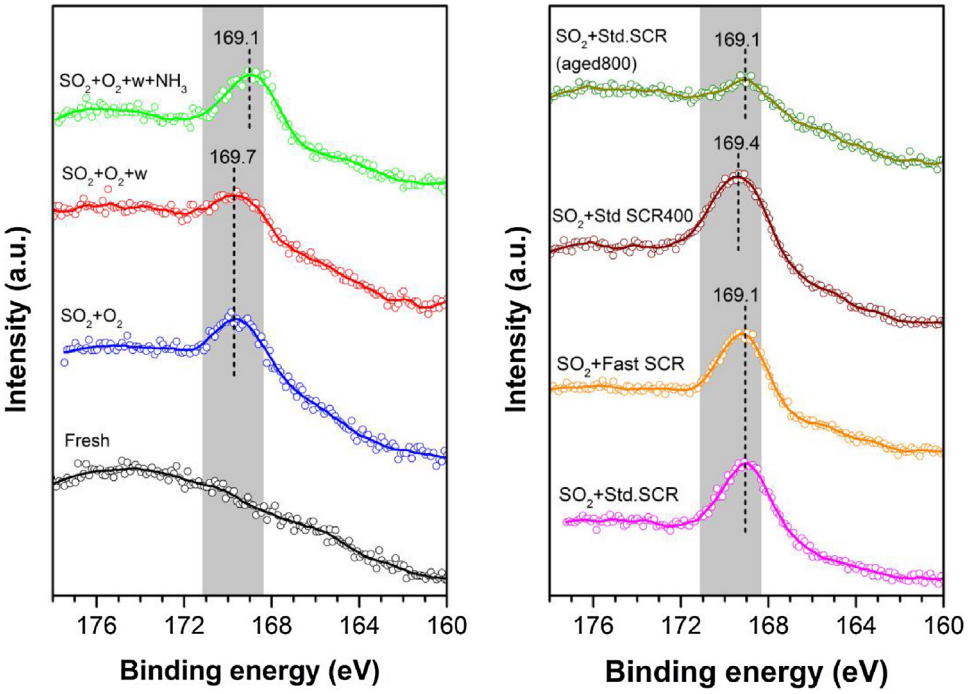

Fig. 3. XPS spectra of sulfur 2p measured on the poisoned and fresh Cu/SSZ-13. The measurement point is shown by (◯) and the solid line indicates the smooth data obtained with the help of the Savitzky-Golay algorithm. The grey area shows the position of sulfates at 171.2–168.4 eV [38]. See Table 1 for details regarding the samples.

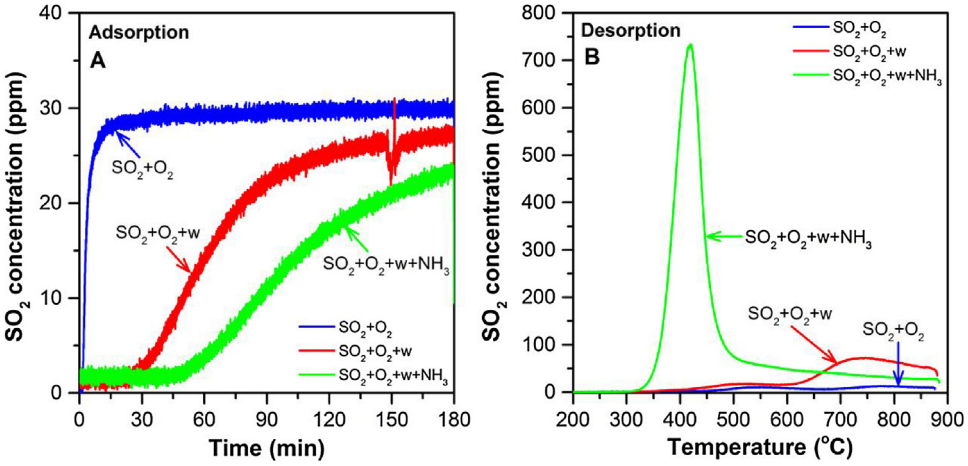

Fig. 4. Outlet concentration of SO_2 during (A) adsorption of 30 ppm SO_2, 8% O_2 (TPD 1) and 30 ppm SO_2, 8% O_2, 5% H_2O (w) (TPD 2) and 30 ppm SO_2, 8% O_2, 5% H_2O (w), 400 ppm NH_3 (TPD 3) at 200 °C for 3 h followed by flushing the catalyst with Ar only for 30 min. SO_2 concentration during temperature ramp (20 °C min^{-1}) is shown in (B).

nium sulfate species which had very likely been formed due to the reaction between sulfur species and ammonia. Indeed, an NH_3 peak was also observed that coincided with the SO_2 peak during the temperature ramp (data not shown here) as a result of the decomposition of the ammonium sulfate species. Our results are in agreement with the TPD results performed by Zhang et al. [22] using Cu/SAPO-34 under dry conditions, where a considerably larger peak of SO_2 was observed that had also occurred at lower temperature as a result of the decomposition of ammonium sulfate or bisulfate species when NH_3 was present during poisoning. These ammonium sulfate species were not observed in the H-SAPO-34 according to Jangjou et al. [39]. Calculation of the mol balance for the results in TPD 3 shows an excellent agreement between the amounts of SO_2 adsorbed and/or consumed during the storage period and the amounts of SO_2 released during the desorption (100% mol balance), which are 0.62 and 0.62 mol SO_2/mol Cu, respectively. Considering that the theoretical stoichiometric ratio between the ammonium sulfate formed and the SO_2 released should be 1:1 and in our case, the mol ratio of SO_2 released/Cu content is less than 1, it is very likely that the ammonium sulfate is attached to the copper sites which is in accordance with the study by Jangjou et al. [39]. Moreover, as discussed earlier in this section, the catalyst is not saturated with sulfur in the outlet part of the monolith as evident from the ICP-SFMS data (see Table 2); thus, the ratio of SO_2/Cu would likely be higher than 0.62 at saturation.

The presence of sulfate species in the sample loaded with sulfur in the presence of NH_3 was also detected during the UV–vis measurement as displayed in Fig. 5A. The center of the broad band at high wave length was observed at around 740 nm for the sample exposed to $SO_2 + O_2 + H_2O + NH_3$, which was at a lower wavelength than the samples without NH_3 exposure. This difference suggests the possibility of the presence of different species during SO_2 expo-

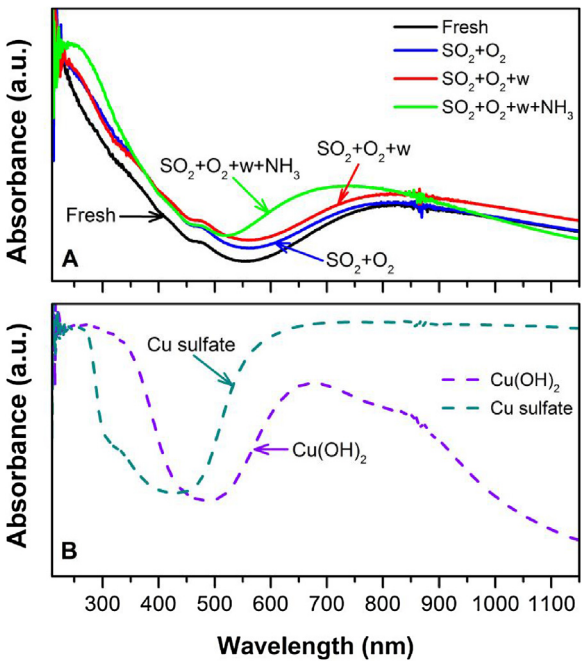

Fig. 5. UV–vis spectra of fresh catalyst and samples that underwent SO_2 storage with ($SO_2 + O_2$) and ($SO_2 + O_2 + H_2O$ (w)) and ($SO_2 + O_2 + H_2O$ + w + NH_3) at 200 °C for 3 h in comparison with $Cu(OH)_2$ and Cu sulfate as the reference material. The gas concentration during storage experiment was 30 ppm SO_2, 8% O_2, 5% H_2O, 400 ppm NH_3 and Ar was used as the inert.

sure in combination with NH_3, which is in accordance with the results from the TPD experiment, where we suggested that ammonium sulfate species might be present. Since this broad peak in the UV–vis spectra refers to the d–d transition of Cu^{2+} ions [33–35] in octahedral coordination [35], it can be inferred that the ammonium sulfate species are attached to the copper sites. In addition, it can be seen from Fig. 5A that the presence of NH_3 during sulfur poisoning resulted in a higher intensity for the peak centered at 220 nm which corresponds to the charge transfer of O → Cu due to the isolated Cu^{2+} than the other samples which might be attributed to the fact that additional sulfate species are found in the sulfur poisoned sample with NH_3 than the latter, which is also seen in the TPD experiment.

From the result of the XPS measurement presented in Fig. 3, it can be seen that the sample exposed to SO_2, O_2 and water in combination with NH_3 showed the sulfate peak at 169.1 eV. Thus, this peak had lower binding energy than the catalysts which had been poisoned with SO_2 in the absence of NH_3 (169.7 eV). The shifted binding energy shown in the XPS spectra is likely due to different sulfate species on these samples. It has been mentioned earlier that the result of the TPD experiment shows that copper sulfate species were formed on the samples exposed to SO_2 without NH_3, whereas ammonium sulfate species preferably exist on the catalyst after it had been poisoned with SO_2 in the presence of NH_3. In addition, the UV–vis spectra were clearly different when sulfur exposure was conducted in the presence of sulfur. Thus, we propose that the shift in binding energy observed during the XPS measurements is owing to the formation of ammonium sulfates and based on the UV–vis data that they are connected to the copper sites.

3.3. *Effect of NO and NO_2*

Under real conditions, the SO_2 poisoning and SCR reaction occur simultaneously; thus, it is important to study the effect of poisoning under standard and fast SCR conditions. The adsorption experiment with 30 ppm SO_2, 8% O_2, 5% H_2O and 400 ppm NH_3 is compared to experiments with SO_2 poisoning under standard SCR (TPD 4, see Table 1) and fast SCR (TPD 5, see Table 1) conditions with the results presented in Fig. 6. As can be seen in Fig. 6A, the amounts of SO_2 consumed were similar among the samples, although a somewhat higher consumption was seen for the case of SO_2 storage under standard SCR conditions. The ICP-SFMS measurement showed a comparable trend for the sulfur storage with NH_3 and under standard SCR conditions, where similar values were received both for the inlet parts (2.2 and 2.3 wt.) and outlet parts (1.4 and 1.4 wt.%). However, for the case of the fast SCR condition, only 2.0 wt.% S was detected in the inlet part which was slightly lower than the other two cases. In addition, the outlet part also had 2.0 % S, showing a more uniform poisoning compared to the poisoning under standard SCR conditions. During the poisoning period, besides the reactions with SO_2 to form ammonium sulfate species, NH_3 also underwent SCR reactions with NO and NO_2; therefore, as shown in Fig. 6B for the cases with NO and NO_2 present, additional NH_3 was consumed compared to the case of adsorption without those gases. It has been observed that for the Cu/CHA catalyst, the rate of reaction of fast SCR is similar to the standard case [14,40]; however, as noted from Fig. 6B and C, more NH_3 and NO were converted during the fast SCR compared to the standard SCR conditions. This could be related to the fact that the fast SCR reaction is less affected by sulfur poisoning than the standard SCR reaction [11,14,15]; thus, it is noticeable in Fig. 6D that the NO_x concentration was higher for the latter. Since less ammonia is available to form ammonium sulfate for fast SCR conditions in the beginning of the monolith, it explains the lower sulfur content. Moreover, the lower sulfur concentration in the inlet part of the monolith results in additional sulfur reaching the outlet part of the monolith during the poisoning phase, something that may explain the higher sulfur concentration in the outlet part of the monolith for fast SCR conditions compared to standard SCR and ammonia oxidation.

As a result of the decomposition of ammonium sulfate species, SO_2 and NH_3 peaks were observed during the temperature ramp (Fig. 7A and B). The peaks for three cases (SO_2 during NH_3 oxidation, under standard SCR and fast SCR conditions) were very similar implying that the rate of ammonium sulfate decomposition is not affected by the presence of NO and NO_2 in the poisoning step. It is worth mentioning that an excellent mole balance between the amount of SO_2 adsorbed and released was noted for all three experiments (100, 99 and 97%, respectively). Moreover, although the ICP-SFMS showed that the position of the sulfur in the monolith varied, the ratio of mol SO_2 desorption/mol of Cu was similar for the three cases; 0.62, 0.65 and 0.60 for the SO_2 TPD during NH_3 oxidation conditions and under standard and fast SCR gas mixture, respectively.

Comparison of the UV–vis spectra between the fresh catalyst and the samples that underwent SO_2 storage with NH_3 as well as under standard and fast SCR conditions is illustrated in Fig. 8A, whereas the lower panel shows the spectra of the reference materials. In line with what was observed in the TPD experiments and ICP measurements, there was no discernible difference between the SO_2 storage with NH_3 and that under standard SCR samples except for the case under fast SCR conditions that had slightly lower intensity at the wavelength range of 870–500 nm than those two samples. However, these three samples had a generally comparable trend implying that the formation of ammonium sulfate species occurred on all samples. This is also supported by the XPS measurement result (Fig. 3) showing that the binding energy of sulfate peaks of the samples stored with SO_2 and NH_3, under standard and fast SCR conditions were very similar, which was around 169.1 eV denoting that the similar species, i.e. ammonium sulfates, existed on all samples.

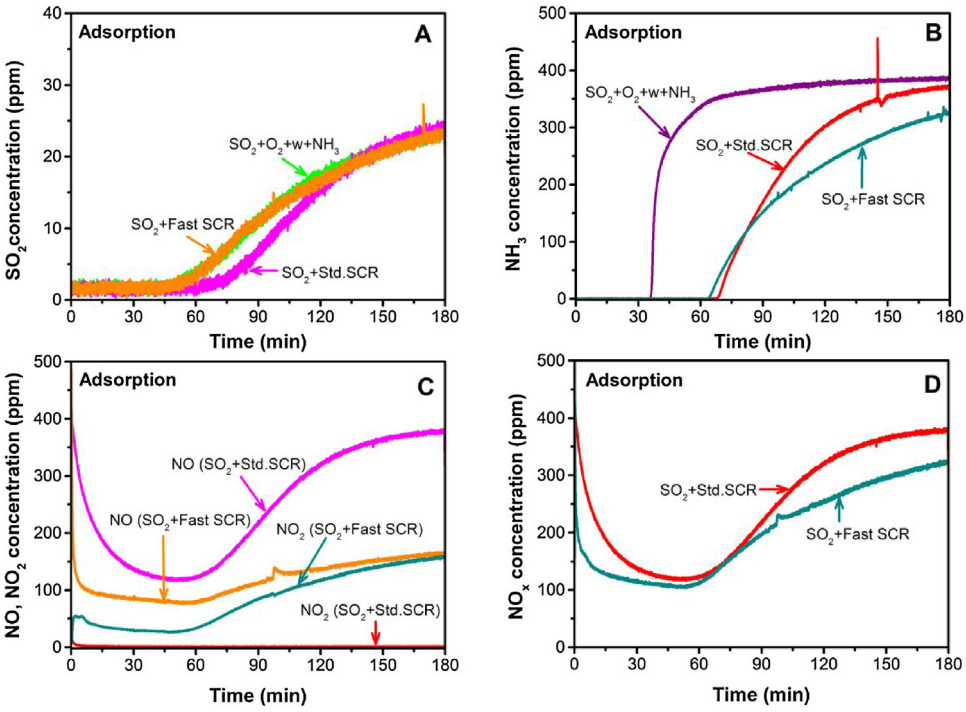

Fig. 6. Concentration of SO_2 (A), NH_3 (B), NO and NO_2 (C), NO_x (D) during adsorption period in which the catalyst was exposed to $SO_2 + O_2 + w + NH_3$ (TPD 3), $SO_2 + O_2 + w + NH_3 + NO$ (SO_2 + Std.SCR, TPD 4), $SO_2 + O_2 + w + NH_3 + NO + NO_2$ (SO_2 + Fast SCR, TPD 5) at 200 °C for 3 h. See Table 1 for gas concentrations.

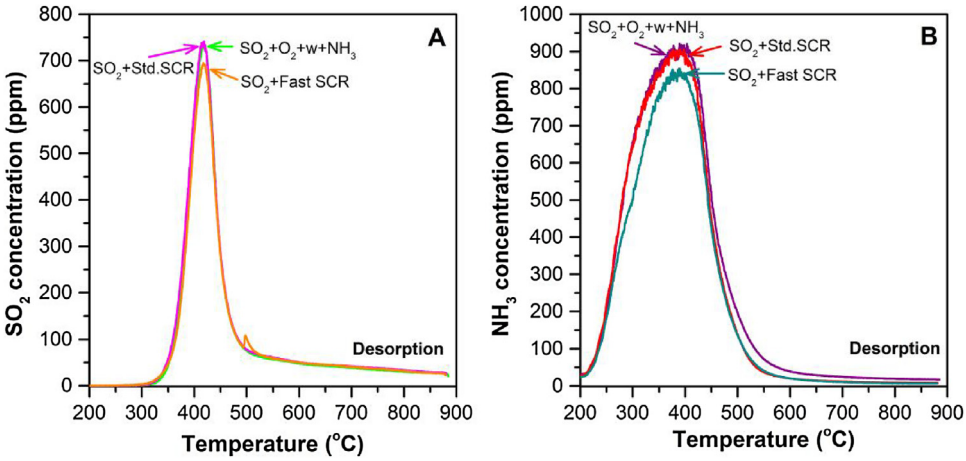

Fig. 7. Concentration of SO_2 (A), NH_3 (B) during temperature ramp (20 °C min^{-1}) after the catalyst was exposed to $SO_2 + O_2 + w + NH_3$ (TPD 3), $SO_2 + O_2 + w + NH_3 + NO$ (SO_2 + Std.SCR, TPD 4) and $SO_2 + O_2 + w + NH_3 + NO + NO_2$ (SO_2 + Fast SCR, TPD 5) at 200 °C for 3 h followed by Ar purge. See Table 1 for gas concentrations.

3.4. *Effect of different ramp conditions*

Besides depending on the SO_2 concentration, the formation and decomposition of sulfates are influenced by O_2 and H_2O because of their abundant presence in diesel exhaust. To investigate this reaction, we performed two experiments of storage SO_2 under SCR conditions (30 ppm SO_2, 8% O_2, 5% H_2O, 400 ppm NH_3, 400 ppm NO) at 200 °C followed by conducting the ramp in different atmospheres, either Ar only (TPD 4, see Table 1) or in the presence of 8% O_2 and 5% H_2O (TPD 6, see Table 1). As can be seen in Fig. 9A and 9B, during the storage period, the outlet concentrations of SO_2, NH_3, and NO were the same, which is expected since the same conditions were used during poisoning. These results show good reproducibility of the experiments. Moreover, when the temperature was linearly increased in the presence of Ar alone; as presented in Fig. 9C, a single SO_2 desorption peak with a maximum at around 420 °C was observed. In addition, a single ammonia peak was also detected during the temperature ramp (Fig. 9D). These peaks were due to the decomposition of ammonium sulfate species which were formed as a result of the reaction of SO_2 and NH_3 during the adsorption period, as discussed in the previous section. In the second case, the ramp was conducted in the presence of O_2 and H_2O resulting in two distinct peaks observed (Fig. 9C). The first peak at around 470 °C was caused by the decomposition of ammonium sulfate species. The reason this peak appeared at higher temperature than in the previous experiment was likely the fact that the presence of O_2 and H_2O during the temperature ramp stabilized the ammonium sulfates and prevented the decomposition. This is supported, as seen in Fig. 9D, by the fact that the NH_3 peak was shifted to higher temperature for the case of O_2 and H_2O in the ramp compared to the ramp in Ar alone (390 versus 415 °C). Moreover, for the experiment with $O_2 + H_2O$ in the ramp, a second peak was noticed at around 675 °C

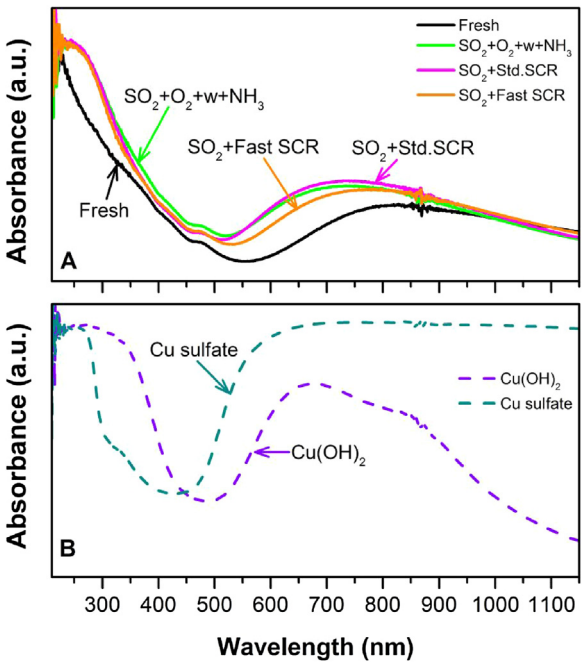

Fig. 8. UV–vis spectra of fresh catalyst and samples that underwent storage experiment with $SO_2 + O_2 + H_2O + NH_3$ (TPD 3), $SO_2 + O_2 + H_2O + NH_3 + NO$ (SO_2 + Std. SCR, TPD 4) and $SO_2 + O_2 + H_2O + NH_3 + NO + NO_2$ (SO_2 + Fast SCR, TPD 5) at 200 °C for 3 h in comparison with $Cu(OH)_2$ and Cu sulfate as the reference materials. Water was denoted by w. The gas concentrations can be found in Table 1.

(Fig. 9C), which was interpreted as copper sulfate species decomposition since it appeared at such high temperature. We propose that during the ramp in oxygen and water, copper sulfates were formed from the ammonium sulfates on the surface, but for the case when ramping in Ar alone, no such transition was possible. It should be mentioned that the experiment with Ar ramp showed an excellent mol balance (99%), which was 0.66 mol SO_2 stored/mol Cu and 0.65 mol SO_2 desorbed/mol Cu. However, for the case of ramp in O_2 and H_2O, the balance between adsorption and desorption of SO_2 was 55%, likely owing to the sulfuric acid formation which was difficult to measure in our system.

3.5. Effect of poisoning temperature

In the real application, the SO_2 poisoning can occur simultaneously with SCR reactions at different temperatures, and we, therefore, studied the effect of poisoning temperature. Two experiments with SO_2 storage under a standard SCR reaction at 200 and 400 °C were performed, after which the catalyst was flushed with O_2 and H_2O for 30 min, followed by a temperature ramp to 900 °C (20 °C min^{-1}) in the same gas mixture. Fig. 10A shows the SO_2 concentration during the storage period where, as expected, less SO_2 was adsorbed/reacted at 400 than 200 °C. These results are in line with the ICP-SFMS results (see Table 2), where 2.3 versus 1.6% sulfur was observed in the front half of the monolith for the 200 and 400 °C experiment, respectively. Further, as presented in Fig. 10B, no NH_3 nor NO was detected in the outlet part of the reactor for the 400 °C experiment due to full conversion of the SCR reaction at this high temperature. Further, during the TPD of the sample that underwent SO_2 storage at 400 °C, the low temperature peak found in the sample with storage at 200 °C disappeared, whereas the high temperature peak was noticeably exactly the same as the sulfur treated sample at 200 °C (see Fig. 10C). These facts indicate that at such a high temperature (400 °C), the formation of ammonium sulfate species during SO_2 poisoning under SCR conditions is hindered. This can be explained by the fact that the SCR reaction was complete at 400 °C (see Fig. 10B), and at this temperature, the SCR zone is in general very short [41]. It is, therefore, probable that sulfur and ammonia do not coexist in most parts of the monolith, thereby hindering ammonium sulfate formation. However, the high

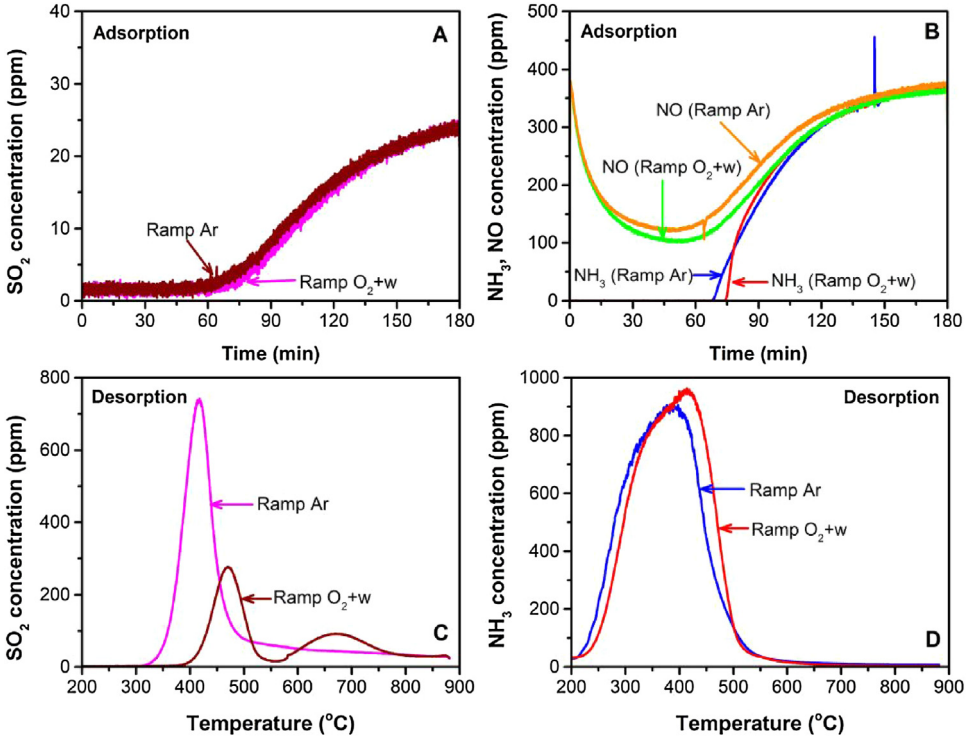

Fig. 9. Concentration of SO_2 (A), NH_3 and NO (B) during adsorption step where the samples were exposed to 30 ppm SO_2, 8% O_2, 5% H_2O, 400 ppm NH_3, 400 ppm NO at 200 °C for 3 h. Concentration of SO_2 (C) and NH_3 (D) during temperature ramp (20 °C min^{-1}) in Ar (TPD 4, see Table 1) and 8% O_2, 5% H_2O (TPD 6).

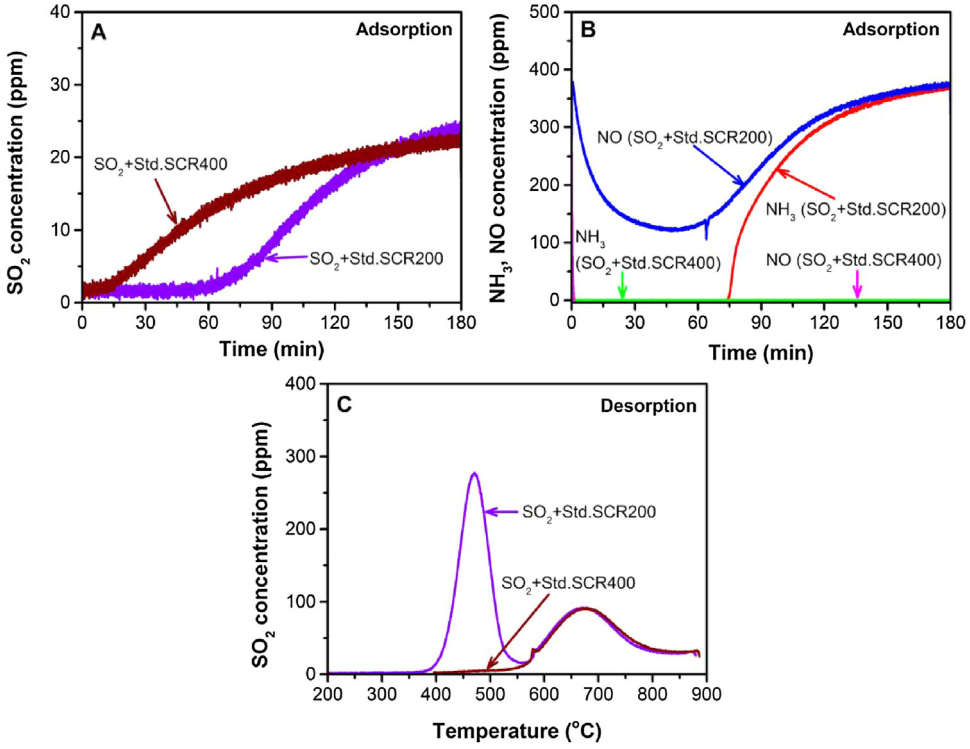

Fig. 10. Comparison of experiments having different temperature of SO_2 adsorption. Concentration of SO_2 (A), NH_3 and NO (B) during the period of exposing the catalyst to 30 ppm SO_2, 8% O_2, 5% H_2O, 400 ppm NH_3, 400 ppm NO for 3 h at 200 or 400 °C followed by O_2 and H_2O purge for 30 min. SO_2 concentration during the temperature ramp (20 °C min^{-1}) in the presence of O_2 and H_2O is shown in (C).

temperature SO_2 peak is attributed to the decomposition of copper sulfate species. It should be noted that the mol balance calculation showed that only 55 and 39% SO_2 consumed were recovered during the desorption period (in the presence of $O_2 + H_2O$) for the samples that underwent 200 and 400 °C SO_2 storage under SCR conditions, respectively. ICP-SFMS was conducted for all samples after the TPD increased to 900 °C and no residual sulfur was found in any of the samples. This was because the desorption step was performed in the presence of O_2 and H_2O; thus, H_2SO_4 was likely formed and as described earlier, this species was difficult to detect in our system. Moreover, Cheng et al. [25] conducted SO_2 poisoning over Cu/zeolites using SO_2, O_2 and H_2O and found the same types of sulfate species at both 200 and 400 °C. We are observing different results because our poisoning is conducted under standard SCR conditions. We therefore propose that under SCR conditions at low temperature, the Cu/SSZ-13 is poisoned by ammonium sulfates on the copper sites, but if poisoning is conducted at high temperature, copper sulfates become the predominant species.

The UV–vis technique was applied to receive additional information concerning the surface species formed and the spectra is presented in Fig. 11. Compared to the fresh sample, as seen in Fig. 11A, the spectra of the 400 °C sulfur stored sample showed higher intensity for the peak centered at around 830 nm which might be due to the presence of Cu sulfate species in accordance with the higher spectra of the Cu sulfate compared with $Cu(OH)_2$, as displayed in Fig. 11B. Meanwhile, the peak associated with the d–d transition of Cu^{2+} ions for the sample treated with SO_2 under SCR conditions at 200 °C was noticeably larger and centered at the wavelength of 740 nm. As mentioned earlier in Section 3.2, the shift of this peak can be correlated with the presence of ammonium sulfate species in this sample. These facts infer that different sulfate species were present in both sulfur poisoned samples which is in accordance with TPD experiments. Moreover, the peak centered at 220 nm for the sulfur treated samples which represent

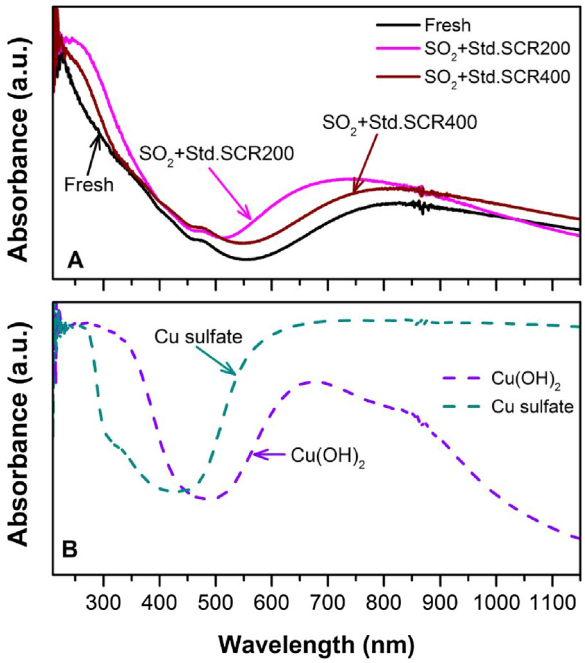

Fig. 11. UV–vis spectra of fresh catalyst and samples that underwent storage experiment with $SO_2 + O_2 + w + NH_3 + NO$ (SO_2 + Std. SCR) at 200 (TPD 4) and 400 °C (TPD 7) for 3 h in comparison with $Cu(OH)_2$ and Cu sulfate as the reference materials. The gas concentrations can be found in Table 1.

the charge metal transfer O → Cu due to the isolated Cu^{2+}, showed higher absorbance intensity for both samples than the fresh case implying that sulfate species affect the isolated Cu^{2+}. Further, the sample which had undergone sulfur treatment under SCR condition at 200 °C displayed higher absorbance intensity of this peak

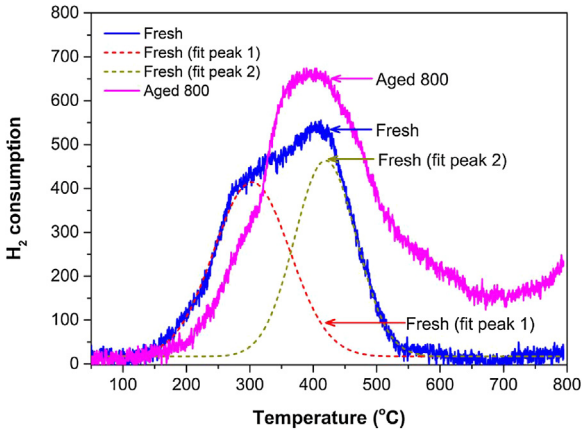

Fig. 12. H_2-TPR profiles for the fresh and 800 °C aged catalysts.

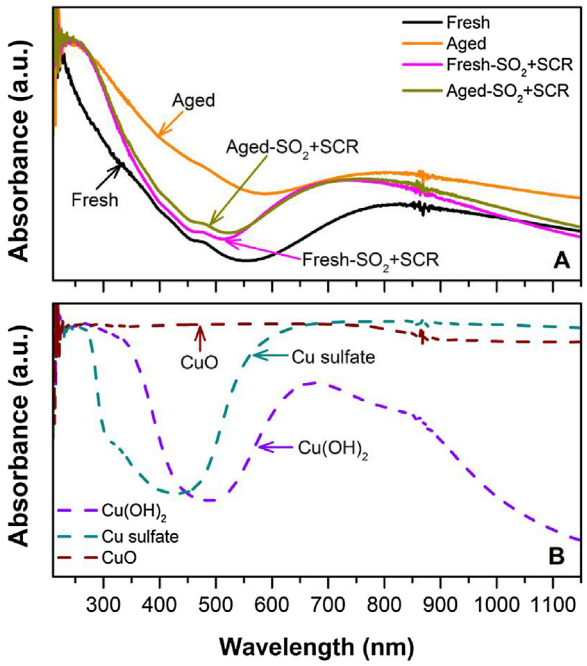

Fig. 13. UV–vis spectra of the fresh and aged samples and the catalysts were exposed to 30 ppm SO_2 under SCR conditions at 200 °C for 3 h (A). The lower panel (B) shows the spectra of $Cu(OH)_2$, Cu sulfate and CuO as reference materials.

denoting that more sulfate species were present than the 400 °C storage sample. This result is in agreement with the sulfur content measurement using the ICP-SFMS technique as listed in Table 2 that 2.3 wt.% sulfur was detected on the inlet part of the sulfur poisoned sample at 200 °C whereas at 400 °C storage, the lower sulfur loading was only 1.6 wt.%.

Characterization using the XPS technique was also performed over the sulfur poisoned samples, with the results displayed in the right panel of Fig. 3. Spectra of the sample of 400 °C sulfur stored under SCR conditions showed a distinct peak at around 169.4 eV due to sulfate species, whereas for the 200 °C sulfur stored sample, the peak was noticeable at 169.1 eV. Moreover, the samples poisoned without the presence of ammonia at 200 °C, i.e. TPD 1 and TPD 2, exhibit the sulfur peak at even higher energies (169.7 eV), see Fig. 3A. Thus, the increased energy of the 400 °C sample compared to 200 °C shows that a larger amount of copper sulfate species in the 400 °C sample, which is in line with UV–vis data. Moreover, the results are also in agreement with the TPD experiments, where during the desorption in the presence of water and O_2, only one peak representing copper sulfate species decomposition was noticeable from the sample with 400 °C sulfur storage, whereas the low temperature sulfur storage sample showed two peaks which may be interpreted as the decomposition of ammonium and copper sulfate species, respectively.

3.6. *Effect of hydrothermal aging*

Hydrothermal aging is one of the critical issues in zeolite-based catalysts; therefore, this section will discuss this point in combination with sulfur poisoning. The hydrothermal aging of the catalyst was performed at 800 °C for 4 h under standard SCR conditions. In order to clarify the transformation of Cu species due to the aging treatment, H_2-TPR experiments were performed with the results presented in Fig. 12. The deconvolution of the main peak in the fresh sample resulted in two peaks, one located at 303 °C (fit peak 1) and the other at 418 °C (fit peak 2), corresponding to the reduction of Cu^{2+} to Cu^{+} which is in good agreement with the calculated H_2 consumption from 50 to 800 °C per mol Cu which was 0.5. The first peak is assigned to the copper in larger cages of CHA structures, whereas the second peak is associated with copper sites occupying the six-membered rings [9,42,43]. According to ab-initio calculations [44], the copper will occupy the sites close to the six-membered rings first and thereafter, the copper start to reside also in the larger cages of the zeolite. The first sites to be occupied (which are close to 6MR) are the most stable positions; therefore, need higher temperature to be reduced, while the copper in larger cages (8MR) are easier to reduce. Since the copper loading is high in the present study (Cu: 7.5 wt.% and Cu/Al: 0.39), both copper types are present.

Further reduction of copper species from Cu^{+} to Cu^{0} occurred at a temperature higher than 800 °C as another reduction peak was observed when the temperature was kept at 800 °C for 40 min. (the result is not shown here). Upon aging, the population of the Cu species at 303 °C decreased and that at 418 °C increased. This result indicates that during the aging treatment, the copper species might have migrated to the more stable position [42,43]. Another possibility is that the migrated copper ions might form metal oxide particles [45]. As can be seen in Fig. 12, the peak area for the aged sample is significantly larger than the fresh case denoting that after the aging treatment, the catalyst becomes more reducible. The same tendency is also applicable to the reduction of Cu^{+} to Cu^{0}, where for the aged catalyst, this reduction started to be observed at lower temperature than for the fresh sample, which is in line with our earlier study [10]. Moreover, a comparison of UV–vis spectra between the fresh and aged catalysts together with the reference materials is presented in Fig. 13. The spectra of the fresh sample show two distinct bands centered at around 830 and 220 nm, indicating the presence of copper hydroxyl species in comparison to the reference materials. The absorbance intensity of the aged sample was noticeably higher than the fresh sample in the 600–300 nm region, and when examining the reference materials (Fig. 13B), it becomes evident that CuO has a very large intensity in this region. Thus, our results show that the aged catalyst contains more copper oxide species, which is in line with our earlier results for Cu/BEA [36].

A comparison of the experimental results for the adsorption-desorption of SO_2 under SCR conditions between the fresh and aged Cu/SSZ-13 catalyst is displayed in Fig. 14. During the adsorption step, the samples were exposed to SO_2, NH_3, NO, O_2 and H_2O at 200 °C for 3 h and as shown in Fig. 14A, a smaller amount of sulfur was stored on the aged catalyst (0.45 mol SO_2/mol Cu) compared to the fresh sample (0.67 mol SO_2/mol Cu). It is worth noting that excellent mol balances were shown during these experiments, where 99 and 98% of the adsorbed SO_2 were recovered during the TPD for the fresh and aged catalyst cases, respectively. Consider-

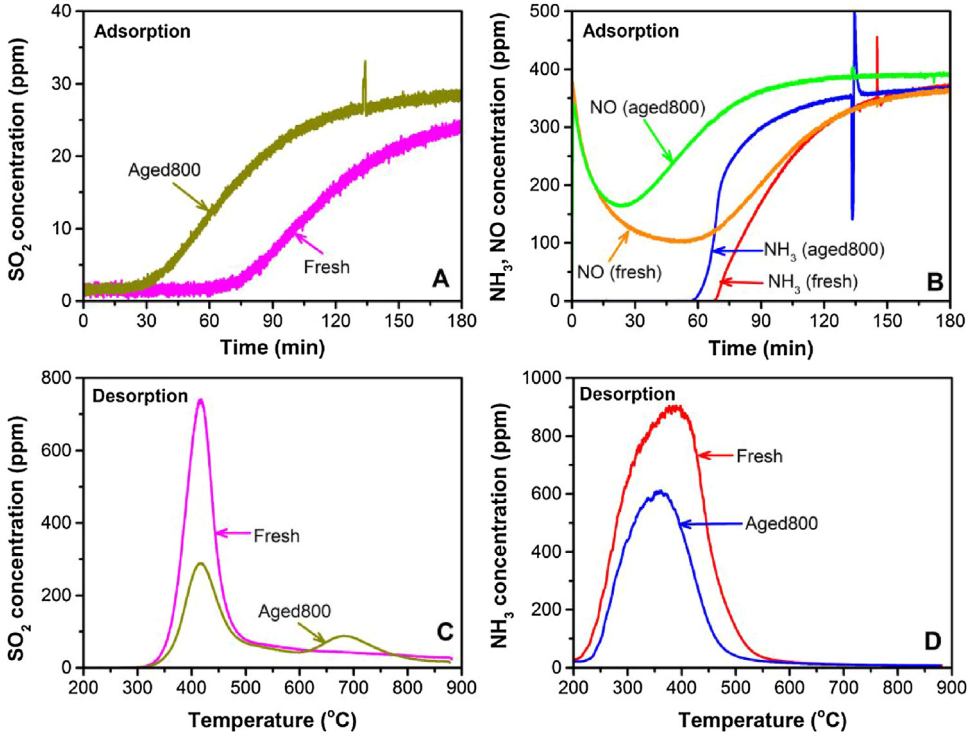

Fig. 14. Concentration of SO_2 (A), NH_3 and NO (B) during adsorption period in which the fresh and aged catalysts were exposed to $SO_2 + O_2 + H_2O + NH_3 + NO$ (SO_2 + Std. SCR) at 200 °C for 3 h followed by Ar flushing for 30 min. The temperature was then increased linearly (20 °C min^{-1}) to 900 °C and the concentration of SO_2 and NH_3 are shown in (C) and (D), respectively. The catalyst aging was conducted in $NH_3 + NO + O_2 + H_2O$ at 800 °C for 4 h. The gas concentration used was 30 ppm SO_2, 8% O_2, 5% H_2O, 400 ppm NH_3 and 400 ppm NO.

ing that the sulfur preferentially poisons copper sites [18,42], the decreasing sulfur storage observed in the TPD experiment suggests that the copper sites to which the sulfur attaches are deactivated by the aging treatment. The UV–vis spectra showed that copper oxides were formed after aging, which might result in the case that some of the copper sites inside the copper oxide particles become inaccessible, which explains the lowered sulfur storage. In line with the result of the adsorption experiments, the XPS spectra presented in Fig. 3 show a similar trend. Both fresh and aged samples which had undergone SO_2 exposure under standard SCR conditions showed a distinct peak at around 169.1 eV due to the presence of ammonium sulfate species. However, it is noticeable that the peak of the aged sample was lower than the poisoned fresh sample implying that the hydrothermal aging decreased the amount of sulfate species formed on the surface. This result was in accordance with the ICP-SFMS measurement (see Table 2) showing that inlet part (also used for XPS) of the aged sample contains lower amount of sulfur than the fresh case (1.4 versus 2.3 wt.%). However, the outlet of the aged monolith contains more sulfur (2.3 wt.%) compared to the inlet part, which is the same value as for the inlet of the non-aged sample (TPD 4, see Table 2). The reason for this could be that the hydrothermal aging was conducted in the flow reactor and that the inlet part of the monolith was more severely aged, resulting in lower sulfur storage in the inlet part. While the outlet part of the monolith probably was less aged, resulting in higher sulfur storage. Moreover, as expected, the hydrothermal treatment had caused a loss of NH_3 storage, as seen in Fig. 14B, which is in good agreement with our previous result using the Cu/BEA catalyst [46]. Moreover, the declining NO_x reduction activity is also evident for the hydrothermally aged sample as shown in Fig. 14B.

Following the Argon flushing for 30 min, the TPD was performed, with the profiles presented in Fig. 14C and Fig. 14D. A huge SO_2 peak at around 420 °C (Fig. 14C), corresponding to the decomposition of ammonium sulfate species, was observed for the poisoned fresh catalyst and upon sulfur poisoning of the hydrothermally aged sample, this peak, although it remained at the same temperature, significantly decreased. This means that the ammonium sulfate production was inhibited for the latter case, which might be attributable to the formation of inaccessible copper sites in copper oxide particles. This is in accordance with the presence of NH_3 peaks as a result of the decomposition of ammonium sulfate species (Fig. 14D). In addition, a new high temperature SO_2 peak at 680 °C was interestingly observed for the hydrothermally aged Cu/SSZ-13 which may be associated with the decomposition of copper sulfate species, something that was also observed for the experiment where poisoning was conducted at 400 °C. This is in line with the study by Xie et al. [47] over CuO/Al_2O_3 where sulfate species usually decompose at temperatures higher than 600 °C. Thus, the TPD experiments provide important insights into the fact that more stable sulfate species is formed when a hydrothermally aged catalyst compared to a fresh catalyst is poisoned with sulfur under SCR conditions.

The UV–vis measurement results over the fresh and hydrothermally aged catalysts as well as after they had undergone SO_2 poisoning under SCR conditions is displayed in Fig. 13A. Compared to the fresh sample without sulfur, the center of the broad band corresponds to d–d transition of Cu^{2+} ions were shifted from 830 to 740 nm for both samples loaded with sulfur indicating the presence of ammonium sulfate species attached to the copper sites, as also seen in the TPD experiments.

To summarize the results for sulfur poisoning of fresh and hydrothermally aged Cu/SSZ-13, we found that less sulfur is stored and desorbed on the hydrothermally aged sample. Moreover, both samples store sulfur in the form of ammonium sulfates, but the hydrothermally aged sample has also formed some copper sulfates already at 200 °C under SCR conditions, which was not the case for the fresh catalyst. Thus, the copper sulfate formation is enhanced

by the presence of copper oxide species on the catalyst, which was observed using UV–vis for the hydrothermally aged sample.

4. Conclusions

The deactivation of Cu/SSZ-13 caused by SO_2 treatment in different gas compositions has been investigated. The TPD technique was employed to characterize different species present during the sulfur poisoning and, in addition, detailed catalyst characterizations with ICP-SFMS, UV–vis and XPS were performed.

During the SO_2 poisoning under dry and lean conditions, two sulfur species assigned to the weakly bound SO_2 and copper sulfate species are present. The sulfur poisoning under humid conditions results in substantially more sulfur species formed compared to that in dry environments. When the SO_2 poisoning was performed in the presence of NH_3, ammonium sulfate species was found on the sample implying that the rate of ammonium sulfate formation is higher than other types of sulfur species. Further, similar TPD profiles were found for SO_2 poisoning during ammonia oxidation, ammonia SCR and fast SCR conditions.

From the experiment of SO_2 poisoning under SCR conditions, it has been revealed that O_2 and H_2O presence during the temperature ramp leads to the formation of more stable copper sulfate species. Moreover, high temperature SO_2 poisoning under SCR conditions results in fewer amounts of sulfur species detected and the observed species are more stable than the species formed during poisoning at lower temperature. Our results indicate that sulfur poisoning under SCR conditions mainly results in ammonium sulfate formation, when performed at 200 °C, whereas mainly copper sulfates are formed after poisoning at 400 °C.

Using H_2 TPR, it was evident that two different copper sites are present on the fresh sample and that the reducibility of the copper increased after the hydrothermal aging treatment at 800 °C. This might be attributable to the copper migration to more stable positions and/or the possibility of the migrated copper forming copper oxide particles. Indeed, the results from the UV–vis experiments clearly showed the formation of copper oxide species. The fresh and hydrothermally aged samples were thereafter poisoned under SCR conditions at 200 °C, showing a lower sulfur adsorption and desorption for the hydrothermally aged sample. Furthermore, an additional high temperature peak was observed for the hydrothermally aged sample, which we assign to the decomposition of copper sulfates. Thus, the copper oxide particles enhanced the copper sulfate formation also under SCR conditions at low temperature (200 °C), while the ion-exchanged Cu mostly formed ammonium sulfates at this temperature.

Acknowledgements

This study was performed at the Chemical Engineering and Competence Centre for Catalysis, Chalmers University and Cummins Inc. The financial support of Cummins Inc. and the Swedish Research Council (621-2011-4860 and 642-2014-5733) is gratefully acknowledged.

References

[1] A.M. Beale, F. Gao, I. Lezcano-Gonzalez, C.H.F. Peden, J. Szanyi, Chem. Soc. Rev. 44 (2015) 7371–7405.
[2] K. Kamasamudram, N.W. Currier, X. Chen, A. Yezerets, Catal. Today 151 (2010) 212–222.
[3] M.P. Ruggeri, I. Nova, E. Tronconi, J.E. Collier, A.P.E. York, Top. Catal. 59 (2016) 875–881.
[4] D.W. Fickel, E. D'Addio, J.A. Lauterbach, R.F. Lobo, Appl. Catal. B 102 (2011) 441–448.
[5] P.N.R. Vennestrøm, A. Katerinopoulou, R.R. Tiruvalam, A. Kustov, P.G. Moses, P. Concepcion, A. Corma, ACS Catal. 3 (2013) 2158–2161.
[6] J.H. Kwak, D. Tran, S.D. Burton, J. Szanyi, J.H. Lee, C.H.F. Peden, J. Catal. 287 (2012) 203–209.
[7] A. Kumar, K. Kamasamudram, A. Yezerets, SAE Int. J. Engines 6 (2013) 680–687.
[8] J.-Y. Luo, A. Yezerets, C. Henry, H. Hess, K. Kamasamudram, H.-Y. Chen, W.S. Epling, Hydrocarbon Poisoning of Cu-Zeolite SCR Catalysts, SAE International, 2012.
[9] J. Hun Kwak, H. Zhu, J.H. Lee, C.H.F. Peden, J. Szanyi, Chem. Commun. 48 (2012) 4758–4760.
[10] K. Leistner, K. Xie, A. Kumar, K. Kamasamudram, L. Olsson, Catal. Lett. (2017), http://dx.doi.org/10.1007/s10562-017-2083-8.
[11] S.J. Schmieg, J.-H. Lee, Evaluation of Supplier Catalyst Formulations for the Selective Catalytic Reduction of NOx With Ammonia, SAE International, 2005.
[12] G. Cavataio, J. Girard, J.E. Patterson, C. Montreuil, Y. Cheng, C.K. Lambert, Laboratory Testing of Urea-SCR Formulations to Meet Tier 2 Bin 5 Emissions, SAE International, 2007.
[13] Y. Cheng, C. Montreuil, G. Cavataio, C. Lambert, SAE Int. J. Fuels Lubricants 1 (2008) 471–476.
[14] K. Wijayanti, K. Leistner, S. Chand, A. Kumar, K. Kamasamudram, N.W. Currier, A. Yezerets, L. Olsson, Catal. Sci. Technol. (2016).
[15] K. Wijayanti, S. Andonova, A. Kumar, J. Li, K. Kamasamudram, N.W. Currier, A. Yezerets, L. Olsson, Appl. Catal B 166–167 (2015) 568–579.
[16] D.W. Brookshear, J.-G. Nam, K. Nguyen, T.J. Toops, A. Binder, Catal. Today 258 (2015) 359–366.
[17] Y. Jangjou, D. Wang, A. Kumar, J. Li, W. Epling, ACS Catal. 6 (6) (2016) 6612–6622.
[18] M. Shen, H. Wen, T. Hao, T. Yu, D. Fan, J. Wang, W. Li, J. Wang, Catal. Sci. Technol. (2015).
[19] Y. Cheng, C. Lambert, D.H. Kim, J.H. Kwak, S.J. Cho, C.H.F. Peden, Catal. Today 151 (2010) 266–270.
[20] H. Hamada, N. Matsubayashi, H. Shimada, Y. Kintaichi, T. Ito, A. Nishijima, Catal. Lett. 5 (1990) 189–196.
[21] K.C. Hass, W.F. Schneider, Phys. Chem. Chem. Phys. 1 (1999) 639–648.
[22] L. Zhang, D. Wang, Y. Liu, K. Kamasamudram, J. Li, W. Epling, Appl. Catal. B 156–157 (2014) 371–377.
[23] C. Wang, J. Wang, J. Wang, T. Yu, M. Shen, W. Wang, W. Li, Appl. Catal. B 204 (2017) 239–249.
[24] Y. Jangjou, D. Wang, A. Kumar, J. Li, W.S. Epling, ACS Catal. 6 (2016) 6612–6622.
[25] Y. Cheng, C. Montreuil, G. Cavataio, C. Lambert, The Effects of SO_2 and SO_3 Poisoning on Cu/Zeolite SCR Catalysts, SAE International, 2009.
[26] A. Kumar, M.A. Smith, K. Kamasamudram, N.W. Currier, H. An, A. Yezerets, Catal. Today 231 (2014) 75–82.
[27] A. Kumar, M.A. Smith, K. Kamasamudram, N.W. Currier, A. Yezerets, Catal. Today 267 (2016) 10–16.
[28] W.K. Su, Z.G. Li, Y.N. Zhang, C.C. Meng, J.H. Li, Catal. Sci. Technol. 7 (2017) 1523–1528.
[29] J.S. McEwen, T. Anggara, W.F. Schneider, V.F. Kispersky, J.T. Miller, W.N. Delgass, F.H. Ribeiro, Catal. Today 184 (2012) 129–144.
[30] K. Leistner, O. Mihai, K. Wijayanti, A. Kumar, K. Kamasamudram, N.W. Currier, A. Yezerets, L. Olsson, Catal.Today 258 (2015) 49–55.
[31] L. Olsson, K. Wijayanti, K. Leistner, A. Kumar, S. Joshi, K. Kamasamudram, N.W. Currier, A. Yezerets, Appl. Catal. B 174–175 (2015) 212.
[32] Z. Huang, Z. Zhu, Z. Liu, Q. Liu, J. Catal. 214 (2003) 213–219.
[33] U. Deka, A. Juhin, E.A. Eilertsen, H. Emerich, M.A. Green, S.T. Korhonen, B.M. Weckhuysen, A.M. Beale, J. Phys. Chem. C 116 (2012) 4809–4818.
[34] S.T. Korhonen, D.W. Fickel, R.F. Lobo, B.M. Weckhuysen, A.M. Beale, Chem. Commun. 47 (2011) 800–802.
[35] T. Zhang, J. Li, J. Liu, D. Wang, Z. Zhao, K. Cheng, J. Li, AIChE J. 61 (2015) 3825–3837.
[36] N. Wilken, R. Nedyalkova, K. Kamasamudram, J. Li, N.W. Currier, R. Vedaiyan, A. Yezerets, L. Olsson, Top. Catal. 56 (2013) 317–322.
[37] B. Jaeckel, R. Hunger, L.J. Webb, W. Jaegermann, N.S. Lewis, J. Phys. Chem. C 111 (2007) 18204–18213.
[38] J.F. Moulder, W.F. Stickle, P.F. Sobol, K.D. Bomben, Handbook of X-Ray Photoelectron Spectroscopy, Physical Electronics Division, Perkin-Elmer Corporation Eden Praire, 1992.
[39] Y. Jangjou, M. Ali, Q. Chang, D. Wang, J. Li, A. Kumar, W.S. Epling, Catal. Sci. Technol. (2016).
[40] P.S. Metkar, M.P. Harold, V. Balakotaiah, Chem. Eng. Sci. 87 (2013) 51–66.
[41] X. Auvray, W. Partridge, J.-S. Choi, J. Pihl, A. Yezerets, K. Kamasamudram, N. Currier, L. Olsson, Appl. Catal. B 126 (2012) 144.
[42] J. Luo, D. Wang, A. Kumar, J. Li, K. Kamasamudram, N. Currier, A. Yezerets, Catal. Today 267 (2016) 3–9.
[43] L. Ma, Y. Cheng, G. Cavataio, R.W. McCabe, L. Fu, J. Li, Chem. Eng. J. 225 (2013) 323–330.
[44] S.A. Bates, A.A. Verma, C. Paolucci, A.A. Parekh, T. Anggara, A. Yezerets, W.F. Schneider, J.T. Miller, W.N. Delgass, F.H. Ribeiro, J. Catal. 312 (2014) 87–97.
[45] Y.J. Kim, J.K. Lee, K.M. Min, S.B. Hong, I.-S. Nam, B.K. Cho, J. Catal. 311 (2014) 447–457.
[46] N. Wilken, K. Wijayanti, K. Kamasamudram, N.W. Currier, R. Vedaiyan, A. Yezerets, L. Olsson, Appl. Catal. B 111–112 (2012) 58–66.
[47] G. Xie, Z. Liu, Z. Zhu, Q. Liu, J. Ge, Z. Huang, J. Catal. 224 (2004) 42–49.